DESY 94–185
CERN–TH. 7478/94
LMU 18/94
October 1994

The process $e^+e^- \to l\bar{l}\,q\bar{q}$ at LEP and NLC

Dima Bardin[1,2], Arnd Leike[3♯] and Tord Riemann[4]

[1] Theoretical Physics Division, CERN, CH–1211 Geneva 23, Switzerland

[2] Theoretical Physics Laboratory, JINR, ul. Joliot-Curie 6, RU–141980 Dubna, Moscow Region, Russia

[3] Lehrstuhl Prof. Fritzsch, Sektion Physik der Ludwig-Maximilians-Universität, Theresienstr. 37, D–80333 München, Germany

[4] DESY–Institut für Hochenergiephysik, Platanenallee 6, D–15738 Zeuthen, Germany

Abstract

The cross sections for the reaction $e^+\,e^- \to l\,\bar{l}\,q\,\bar{q}$ and for similar four fermion production processes at LEP 1, LEP 2 and the NLC are calculated. Due to the extraordinary symmetry properties of the process, very compact analytical formulae describe the double differential distributions in the invariant masses of the $l\bar{l}$ and $q\bar{q}$ pairs. The total cross sections may be obtained with two numerical integrations.

email: bardindy@cernvm.cern.ch, leike@cernvm.cern.ch, riemann@ifh.de

♯ Supported by the German Federal Ministry for Research and Technology under contract No. 05 GMU93P.

1 Introduction

At LEP 1 energies, few events of electron positron annihilation into four fermions, $e^+e^- \to 4f$, have been observed [1] although $4f$ production is extremely suppressed compared to fermion pair production. The $4f$ production is also interesting as a background contribution to light Higgs searches [2] with the associated ZH production. The strong kinematical suppressions are hoped to become overcompensated by the rising number of Z bosons being produced at LEP 1.

Above the production thresholds for gauge boson pairs, four fermion production is predicted by the Standard Model to be one of the most frequent annihilation processes. It will allow to study further details of the gauge boson properties; and the search for Higgs boson signals from the Bjorken process will be one of the challenges of LEP 2.

Several Monte Carlo approaches to the complete description of $4f$ production have been developed [3, 4, 5, 6] while we are performing a program of *semi-analytical* calculations [7, 8, 9]. Although the treatment of even the simplest final states is technically involved we got encouraging results for off shell W pair production [7, 8] and the Bjorken process (off shell ZH production) [9]. Some general remarks on $4f$ production and numerical comparisons may be found in [6, 8, 10]. The neutral current (NC) channels for $4f$ final states are classified in table 1. The four different event classes are discussed in [8]. Higgs boson exchange has been excluded; this is a very good approximation if one doesn't perform a dedicated Higgs search [9].

In this article, we deal with the simplest event class marked in **boldface**. It comprises final states which do neither contain electrons (positrons), electron (anti)neutrinos, nor identical fermions and cannot be produced by charged current interactions.

Our calculation covers the following *observable* final states:

(i) $[\mu\bar{\mu}, \tau\bar{\tau}]$,

(ii) $[l\bar{l}, b\bar{b}]$, $[l\bar{l}, c\bar{c}]$, $[l\bar{l}, (u\bar{u} + d\bar{d} + s\bar{s} + c\bar{c} + b\bar{b})]$,

(iii) $[b\bar{b}, c\bar{c}]$,

where $l = \mu, \tau$. Other reactions of table 1, e.g. those with ν_τ and ν_μ pairs, may also be calculated with the below formulae but are not observable due to the admixture of other final states, here e.g. ν_e pairs. The latter belong to another, much more complicated type of reaction.

In section 2, the calculation is shortly described. Section 3 contains the main result: the analytical formulae for the invariant fermion pair mass distributions. In section 4 we discuss numerical results.

	$\bar{d}d$	$\bar{u}u$	$\bar{e}e$	$\bar{\mu}\mu$	$\bar{\nu}_e\nu_e$	$\bar{\nu}_\mu\nu_\mu$
$\bar{d}d$	4·16	*43*	48	**24**	21	**10**
$\bar{s}s, \bar{b}b$	**32**	*43*	48	**24**	21	**10**
$\bar{u}u$	*43*	4·16	48	**24**	21	**10**
$\bar{e}e$	48	48	4·36	48	*56*	20
$\bar{\mu}\mu$	**24**	**24**	48	4·12	19	*19*
$\bar{\tau}\tau$	**24**	**24**	48	**24**	19	**10**
$\bar{\nu}_e\nu_e$	21	21	*56*	19	4·9	12
$\bar{\nu}_\mu\nu_\mu$	**10**	**10**	20	*19*	12	4·3
$\bar{\nu}_\tau\nu_\tau$	**10**	**10**	20	**10**	12	**6**

Table 1: *Number of Feynman diagrams for 'NC' type final states.*

2 Feynman diagrams, phase space, and cross section

The reaction

$$e^+e^- \to l\bar{l} + b\bar{b} \tag{1}$$

is representative for the class of reactions considered here. It is described by 24 Feynman diagrams with six different topologies which we will call `crab` diagrams and `deer` diagrams; see figures 1 and 2. If there are two quark pairs in the final state, the `deers` may also contain gluon exchange. This will be discussed later.

We parametrize the eightdimensional four particle phase space as follows:

$$\begin{aligned} d\Gamma &= \prod_{i=1}^{4} \frac{d^3p_i}{2p_i^0} \times \delta^4(k_1 + k_2 - \sum_{i=1}^{4} p_i) \\ &= 2\pi \frac{\sqrt{\lambda(s, s_1, s_2)}}{8s} \frac{\sqrt{\lambda(s_1, m_1^2, m_2^2)}}{8s_1} \frac{\sqrt{\lambda(s_2, m_3^2, m_4^2)}}{8s_2} ds_1 ds_2 d\cos\theta d\Omega_1 d\Omega_2, \end{aligned} \tag{2}$$

with the usual definition of the λ function,

$$\lambda(a, b, c) = a^2 + b^2 + c^2 - 2ab - 2ac - 2bc, \tag{3}$$

$$\lambda \equiv \lambda(s, s_1, s_2). \tag{4}$$

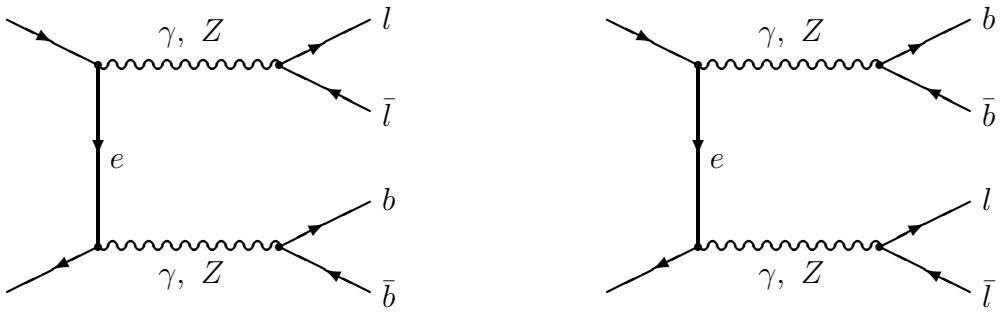

Figure 1: *The* `crab` *diagrams.*

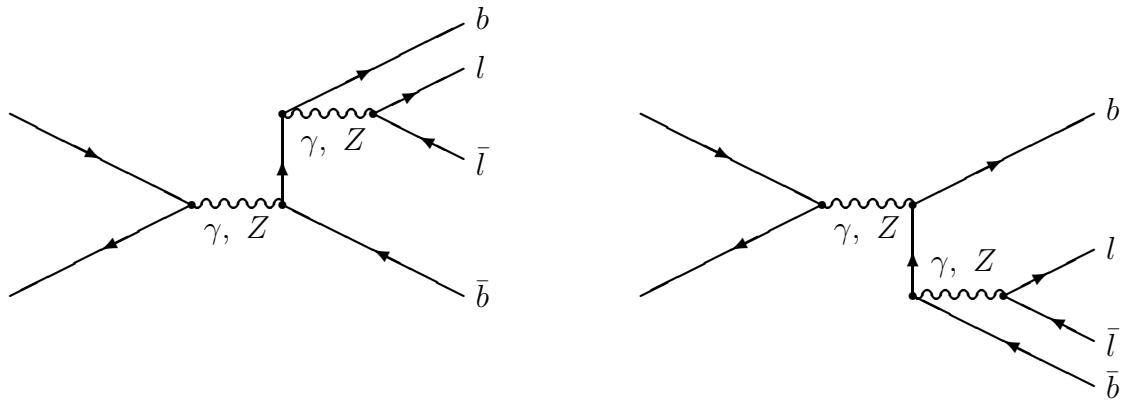

Figure 2: *The* `b-deer` *diagrams. The* `l-deers` *may be obtained by interchanging the leptons with the quarks.*

In (2), the rotation angle around the beam axis has been integrated over already. Variables k_1 and k_2 are the four-momenta of electron and positron and p_1, p_2, p_3, p_4 are those of the final state particles $f_1, \bar{f}_1, f_2, \bar{f}_2$ with $p_i^2 = m_i^2$. All fermion masses are neglected compared to the invariants s, s_1, and s_2 [1]:

$$s = (k_1 + k_2)^2, \quad s_1 = (p_1 + p_2)^2, \quad s_2 = (p_3 + p_4)^2. \tag{5}$$

The angle θ is located between the vectors $(\vec{p_1} + \vec{p_2})$ and $\vec{k_1}$. The spherical angle of $\vec{p_1}$ ($\vec{p_3}$) in the rest frame of the compound $[f_1\bar{f}_1]$ ($[f_2\bar{f}_2]$) is Ω_1 (Ω_2): $d\Omega_i = d\cos\theta_i d\phi_i$. The kinematical ranges of the integration variables are:

$$\begin{aligned} (m_1+m_2)^2 \le s_1 \le (\sqrt{s} - m_3 - m_4)^2 \quad , \qquad & (m_3+m_4)^2 \le s_2 \le (\sqrt{s} - \sqrt{s_1})^2, \\ -1 \le \cos\theta,\ \cos\theta_1,\ \cos\theta_2 \le 1 \quad , \qquad & 0 \le \phi_2, \phi_1 \le 2\pi. \end{aligned} \tag{6}$$

We are interested in analytical formulae for distributions in invariant masses of fermion pairs. Thus, we have to integrate analytically over the five angular variables in (2). The matrix elements squared have been determined by two independent calculations. One of them used the symbolic manipulation program `FORM` [11]. The other one determined the squared matrix elements with `CompHEP` [12] and continued then with the angular integrations in a different `FORM` program.

The total cross section may be written as a sum of six contributions:

$$\sigma(s) = \int_{\bar{s}_1}^{s} ds_1 \int_{\bar{s}_2}^{(\sqrt{s}-\sqrt{s_1})^2} ds_2 \sum_{k=1}^{6} \frac{d^2\sigma_k(s, s_1, s_2)}{ds_1 ds_2}. \tag{7}$$

In (7) we allow for lower cuts on the invariant masses. Index $k = 1$ corresponds to the square of the sum of the `crabs`, and $k = 2, 3$ to that of the `b-deers` and `l-deers`. Further, $k = 4, 5$ and 6 correspond to the interferences between `l-deers` and `b-deers`, between `crabs` and `b-deers`, and between `crabs` and `l-deers`, respectively.

3 The cross section

All the diagrams which mediate process (1) have a common topology. They contain three fermion antifermion pairs connected by neutral gauge bosons. Two of the fermion pairs couple to a gauge boson while the third one couples to two gauge bosons with a fermion propagator between them. In this sense, there is only one generic topology, the `deer` topology, and the `crab` diagrams may be considered as the `e-deers` in a crossed channel.

Our choice of coordinates takes the above symmetry into account. All the 300 interferences between the 24 diagrams may be reduced to two generic ones. This may be achieved by grouping the diagrams in the calculation as is indicated in the figures, i.e. in sums of `deers` of the same type. A tremendous reduction of terms arises during the calculation leading to an extremely compact result.

The first generic interference is known from off shell Z boson pair production [8]. It is the square of the `crab` diagrams or generally of same-type `deers`. The three cases differ from each other by permutations of the invariant masses and couplings. The second generic kinematic function is due to the interference of different types of `deers`. Again, three such cases are related by permutations.

[1] An exception arises if there are photon propagators $1/s_i$ involved and if no cut is applied. In this case, the finite masses of the fermions yield non-logarithmic contributions of order $\mathcal{O}(1)$. These may be taken into account by replacing in (2) the $\sqrt{1-4m_f^2/s_i}$ by $\sqrt{1-4m_f^2/s_i}\,(1+2m_f^2/s_i)$ (instead of neglecting m_f^2/s_i).

Hence, the complete cross section can be written as a sum of six basic interferences between the three basic sets of diagrams.

The cross section from the two `crab` diagrams alone reads as follows:

$$\frac{d^2\sigma_1(s;s_1,s_2)}{ds_1 ds_2} = \frac{\sqrt{\lambda}}{\pi s^2} C_{422}(e,s;l,s_1;b,s_2)\mathcal{G}_{422}(s;s_1,s_2)\ . \tag{8}$$

This expression factorizes into a function of couplings and a kinematical $\mathcal{G}$-function and is symmetric in s_1 and s_2; the latter depends exclusively on the virtualities[2]:

$$\mathcal{G}_{422}(s;s_1,s_2) = \frac{s^2+(s_1+s_2)^2}{s-s_1-s_2}\mathcal{L}(s;s_1,s_2) - 2, \tag{9}$$

with

$$\mathcal{L}(s;s_1,s_2) = \frac{1}{\sqrt{\lambda}}\ \ln\frac{s-s_1-s_2+\sqrt{\lambda}}{s-s_1-s_2-\sqrt{\lambda}}. \tag{10}$$

The couplings and gauge boson propagators are contained in the following C-factor:

$$\begin{aligned} C_{422}(e,s;f_1,s_1;f_2,s_2) &= \frac{2s_1s_2}{(6\pi^2)^2}\,\Re e \sum_{V_i,V_j,V_k,V_l=\gamma,Z} \frac{1}{D_{V_i}(s_1)}\frac{1}{D_{V_j}(s_2)}\frac{1}{D^*_{V_k}(s_1)}\frac{1}{D^*_{V_l}(s_2)} \\ &\times\ [L(e,V_i)L(e,V_k)L(e,V_j)L(e,V_l) + R(e,V_i)R(e,V_k)R(e,V_j)R(e,V_l)] \\ &\times\ [L(f_1,V_i)L(f_1,V_k) + R(f_1,V_i)R(f_1,V_k)]\,N_c(f_1) \\ &\times\ [L(f_2,V_j)L(f_2,V_l) + R(f_2,V_j)R(f_2,V_l)]\,N_c(f_2). \end{aligned} \tag{11}$$

The conventions for the left- and right-handed couplings between vector bosons and fermion f are:

$$L(f,\gamma) = R(f,\gamma) = \frac{eQ_f}{2}, \tag{12}$$

$$L(f,Z) = \frac{e}{4s_Wc_W}\left(2I_3^f - 2Q_fs_W^2\right), \quad R(f,Z) = \frac{e}{4s_Wc_W}\left(-2Q_fs_W^2\right). \tag{13}$$

Here, we use $e=\sqrt{4\pi\alpha}$, $Q_e=-1$, $I_3^e=-\frac{1}{2}$, and $s_W^2 = 1-M_W^2/M_Z^2$. Further, we choose $\alpha/\pi = \sqrt{2}M_W^2s_W^2G_\mu/\pi^2$. The numerical input for the figures is $G_\mu = 1.16639\times10^{-5}$, $M_W = 80.220$ GeV, $M_Z = 91.173$ GeV, $\Gamma_Z = 2.497$ GeV. The colour factor $N_c(f)$ is equal to unity for leptons and three for quarks. The propagators are

$$D_V(s) = s - M_V^2 + i\sqrt{s}\,\Gamma_V(s). \tag{14}$$

For the photon, it is $M_\gamma = \Gamma_\gamma = 0$. The Z width function depends on the decay channels which are open at a given energy; at the Z peak and above, a good approximation is $\Gamma_Z(s) = \sqrt{s}\,\Gamma_Z/M_Z$. The D^* is the complex conjugate of the propagator D. The resonating behaviour of the cross section depends on the arguments of the function C_{422}. With e.g. all $V_i = Z$ in (11), one selects the off shell Z pair production diagrams squared (see figure 1), whose contribution is proportional to two Breit Wigner resonance factors,

$$C_{422} = \ldots + 2\left[L^4(e,Z) + R^4(e,Z)\right]\ \frac{1}{\pi}\,\frac{\sqrt{s_1}\,\Gamma_Z(f_1)}{|D_Z(s_1)|^2}\ \frac{1}{\pi}\,\frac{\sqrt{s_2}\,\Gamma_Z(f_2)}{|D_Z(s_2)|^2}, \tag{15}$$

[2] This function may be found in the article [13] on electromagnetic pair production and also in [14] where extra neutral gauge boson production is studied.

with

$$\lim_{\Gamma\to 0}\frac{1}{\pi}\frac{\sqrt{s}\,\Gamma}{|D(s)|^2}=\delta(s-M^2). \tag{16}$$

The cross section contributions σ_2 from the square of the `b-deers` and σ_3 of the `l-deers` are:

$$\frac{d^2\sigma_2(s;s_1,s_2)}{ds_1ds_2} = \frac{\sqrt{\lambda}}{\pi s^2}C_{422}(b,s_2;e,s;l,s_1)\mathcal{G}_{422}(s_2;s,s_1), \tag{17}$$

$$\frac{d^2\sigma_3(s;s_1,s_2)}{ds_1ds_2} = \frac{\sqrt{\lambda}}{\pi s^2}C_{422}(l,s_1;b,s_2;e,s)\mathcal{G}_{422}(s_1;s_2,s). \tag{18}$$

In these contributions the potential resonance behaviour is in the variables s and s_1 *or* s_2, respectively.

Besides the above moduli squares, there are interferences among the three different groups of diagrams. The interference between `l-deers` and `b-deers` is again symmetric in the last two arguments:

$$\frac{d^2\sigma_4(s;s_1,s_2)}{ds_1ds_2} = \frac{\sqrt{\lambda}}{\pi s^2}C_{233}(e,s;l,s_1;b,s_2)\mathcal{G}_{233}(s;s_1,s_2), \tag{19}$$

with the kinematical function $\mathcal{G}_{233}(s;s_1,s_2)$,

$$\begin{aligned}\mathcal{G}_{233}(s;s_1,s_2) = \frac{3}{\lambda^2}\Big\{&\mathcal{L}(s_2;s,s_1)\mathcal{L}(s_1;s_2,s)4s\left[ss_1(s-s_1)^2+ss_2(s-s_2)^2+s_1s_2(s_1-s_2)^2\right]\\
&+(s+s_1+s_2)\Big[\mathcal{L}(s_2;s,s_1)2s\left[(s-s_2)^2+s_1(s-2s_1+s_2)\right]\\
&\quad+\mathcal{L}(s_1;s_2,s)2s\left[(s-s_1)^2+s_2(s+s_1-2s_2)\right]\\
&\quad+5s^2-4s(s_1+s_2)-(s_1-s_2)^2\Big]\Big\}.\end{aligned} \tag{20}$$

For $\lambda\to 0$ it remains finite, $\mathcal{G}_{233}(s;s_1,s_2)\to -3\ (3s-s_1-s_2)/\ [(s+s_1-s_2)(s+s_2-s_1)]$. The C factor with couplings and propagators is:

$$\begin{aligned}C_{233}(e,s;f_1,s_1;f_2,s_2) = &\frac{2ss_1s_2}{(6\pi^2)^2}\Re e\sum_{V_i,V_j,V_k,V_l=\gamma,Z}\frac{1}{D_{V_i}(s)}\frac{1}{D_{V_j}(s_2)}\frac{1}{D^*_{V_k}(s)}\frac{1}{D^*_{V_l}(s_1)}\\
&\times\ [L(e,V_i)L(e,V_k)+R(e,V_i)R(e,V_k)]\\
&\times\ [L(f_1,V_i)L(f_1,V_j)L(f_1,V_l)-R(f_1,V_i)R(f_1,V_j)R(f_1,V_l)]\,N_c(f_1)\\
&\times\ [L(f_2,V_j)L(f_2,V_k)L(f_2,V_l)-R(f_2,V_j)R(f_2,V_k)R(f_2,V_l)]\,N_c(f_2).\end{aligned} \tag{21}$$

Both final fermion traces must couple to an axial current. Otherwise the contribution vanishes due to the Furry theorem.

The remaining two interferences σ_5 among `crabs` and `b-deers` and σ_6 among `crabs` and `l-deers` are:

$$\frac{d^2\sigma_5(s;s_1,s_2)}{ds_1ds_2} = \frac{\sqrt{\lambda}}{\pi s^2}C_{233}(l,s_1;b,s_2;e,s)\mathcal{G}_{233}(s_1;s_2,s), \tag{22}$$

$$\frac{d^2\sigma_6(s;s_1,s_2)}{ds_1ds_2} = \frac{\sqrt{\lambda}}{\pi s^2}C_{233}(b,s_2;e,s;l,s_1)\mathcal{G}_{233}(s_2;s,s_1). \tag{23}$$

The interferences of different-type `deers` may become resonating only in the first argument of the function $C_{233}(f_1, s_1; f_2, s_2; f_3, s_3)$.

At the end of this section, we would like to comment on processes with four quarks in the final state. In this case, besides photons and Z bosons also gluons may be exchanged in the `deer` diagrams while the `crab` contribution σ_1 remains unchanged. The gluonic contributions to σ_5 and σ_6 vanish due to the colour trace, but σ_2, σ_3, and σ_4 get additional contributions. The sum over gauge bosons in the C-functions in (17)–(19) extends now also over gluons. The gluon couplings to quarks are

$$L(q, g) = R(q, g) = \frac{1}{2}\sqrt{4\pi\alpha_s}, \tag{24}$$

and the gluon propagator looks like the photon propagator. Further, the colour factor $N_c(f_1)N_c(f_2)$ has to be replaced by a factor of $(N_c^2 - 1)/4 = 2$ for all interferences with *two* gluons and by a zero if only *one* gauge boson is a gluon.

If one observes two hadron jets without flavour tagging, then there are also contributions from diagrams with a three gluon vertex which have to be added incoherently. If the quark types may be tagged, such contributions are of higher order and may be neglected.

4 Results

Numerical comparisons have been performed for $e^+e^- \to \mu^+\mu^- b\bar{b}$ and $e^+e^- \to \nu_\mu\bar{\nu}_\mu b\bar{b}$ at LEP 2 energies with a Monte Carlo approach [6]; see also [10]. The agreement is within 0.2% and is limited by the numerical accuracy of the Monte Carlo program.

There are two different energy regions of physical interest. At LEP 1, among others the cases (i) and (ii–3) (see Introduction) are observed [1] and case (ii–1) is searched for as a Higgs boson signal [2][3]. While, at higher energies the most interesting channel is (ii–1).

In figure 3, the cross sections of cases (i), (ii–1), and (ii–3) are shown at LEP 1 energies. We assume cuts being applied to the final state fermion pairs. For illustrational purposes, cross section (i) is shown also without cut. The cross section is sensitive to this due to the diagrams with photon exchange which are extremely enhanced when their virtualities approach to $4m_f^2$. The cross sections are peaking at $\sqrt{s} = M_Z$, if the non-resonating gauge boson is a photon with a small virtuality. In [4], partial widths of the Z boson into $4f$ final states are systematically studied. Having in mind that the production cross sections are proportional to them at the Z peak, one may compare corresponding ratios with each other. We have done this in the massless limit for the cases $[\mu\bar{\mu}, \tau\bar{\tau}]$, $[\mu\bar{\mu}, b\bar{b}]$, $[\mu\bar{\mu}, (u\bar{u} + d\bar{d} + s\bar{s} + c\bar{c} + b\bar{b})]$ and found agreement within 1 % which is the accuracy of the numbers quoted in [4].

Figure 4 shows final states (i), (ii–1), and (iii–1) in the energy region $\sqrt{s} \sim 100 - 500$ GeV. Again, in one case the influence of the cuts on the invariant masses is exhibited. As to be expected, there are pronounced thresholds at the onset of on shell Z pair production. At higher energies, the cross sections fall monotonically. In the figure, we show also a four quark final state. The strong coupling constant α_s is a function of the virtualities s_1 or s_2 (and in some interferences of both) and may not be reasonably chosen here. For the illustrational purposes, we fixed it somehow arbitrarily at $\alpha_s = 0.2$; this corresponds to smaller values of the gluon virtualities which give the dominant contributions.

We also should mention that there are substantial radiative corrections to $4f$ production. The bulk of them is known to arise from initial state photonic bremsstrahlung. It may be easily taken

[3] We did not perform a dedicated comparison with the experimental results at LEP 1 [1] since the applied cuts are different from ours; our predictions agree roughly with them.

Figure 3: *Total cross sections $\sigma(e^+e^- \to 4f)$ at LEP 1 energies. The following cuts are applied: $E_{q\bar{q}}, E_{\mu\bar{\mu}} > 2$ GeV, $E_{\tau\bar{\tau}} > 2m_\tau$, $E_{c\bar{c}} > 5$ GeV, $E_{b\bar{b}} > 20$ GeV.*

Figure 4: *Total cross sections $\sigma(e^+e^- \to 4f)$ at LEP 2 and NLC energies. The following cuts are applied: $E_{\mu\bar{\mu}} > 2$ GeV, $E_{\tau\bar{\tau}} > 2m_\tau$, $E_{c\bar{c}} > 5$ GeV, $E_{b\bar{b}} > 20$ GeV.*

into account with a convolution formula which is well known from the Z line shape [6, 8]. These corrections amount to – $\mathcal{O}(15\%)$ around the peaks and are smaller elsewhere, becoming positive (and cut dependent) in the radiative tail regions. Since all these effects are well known we do not go into numerical details on them. Our Fortran program `4fAN` may take them into account.

To summarize, we performed the first complete semi-analytical calculation of neutral current four fermion production. We obtained, for the simplest topology, extremely compact analytical results for the two-dimensional invariant mass distributions. The remaining two integrations are fast and numerically stable. Polarized beams and the inclusion of heavy neutral gauge bosons are also described by our formulae.

Acknowledgement

We would like to thank F. Berends for discussions, hints, and a numerical comparison.

References

[1] DELPHI Collab., P. Abreu et al., *Nucl. Phys.* **B403** (1993) 299;
ALEPH Collab., D. Buskulic et al., *Phys. Letters* **B313** (1993) 299;
OPAL Collab., R. Akers et al., CERN–PPE/93–145 (1993);
L3 Collab., A. Adam et al., *Phys. Letters* **B321** (1994) 283;
and references therein.

[2] See e.g.: J.P. Martin, Invited talk at Les Rencontres de Physique de la Vallee d'Acoste, Results and Perspectives in Particle Physics, March 1994, La Thuile, preprint LYCEN/9425 (May 1994), and references therein.

[3] F.A. Berends, P.H. Daverveldt and R. Kleiss, *Nucl. Phys.* **B253** (1985) 441; *Comput. Phys. Commun.* **40** (1986) 285;
J. Hilgart, R. Kleiss and F. le Diberder, *Comput. Phys. Commun.* **75** (1993) 191.

[4] E.W.N. Glover, R. Kleiss and J.J. van der Bij, *Z. Physik* **C47** (1990) 435;

[5] E. Boos, M. Sachwitz, H. Schreiber and S. Sichanin, *Z. Physik* **C61** (1994) 675;
M. Dubinin, V. Edneral, Y. Kurihara and Y. Shimizu, *Phys. Letters* **B329** (1994) 379.

[6] F.A. Berends, R. Kleiss and R. Pittau, Nucl. Phys. **B424** (1994) 308; Nucl. Phys. **B426** (1994) 344;
R. Pittau, *Phys. Letters* **B335** (1994) 490.

[7] D. Bardin, M. Bilenky, A. Olchevski and T. Riemann, *Phys. Letters* **B308** (1993) 403.

[8] D. Bardin, M. Bilenky, D. Lehner, A. Olchevski and T. Riemann, Contribution to the Zeuthen Workshop on Elementary Particle Theory – Physics at LEP200 and Beyond, Teupitz, Germany, April 1994, preprint CERN-TH. 7295/94 (1994) (hep-ph/9406340); to appear in the proceedings.

[9] D. Bardin, A. Leike and T. Riemann, Contribution to the Zeuthen Workshop on Elementary Particle Theory – Physics at LEP200 and Beyond, Teupitz, Germany, April 1994, preprint DESY 94-097 (1994) (hep-ph/9406273); to appear in the proceedings.

[10] F.A. Berends, R. Kleiss and R. Pittau, contribution to the ICHEP94, July 1994, Glasgow, UK, to appear in the proceedings.

[11] J.A.M. Vermaseren, *Symbolic Manipulation with* `FORM`, CAN, Amsterdam, 1991.

[12] `CompHEP`, E. Boos et al., KEK preprint 92–47 (1992) and references therein.

[13] V. Baier, V. Fadin and V. Khoze, *Sov. Phys. JETP* **23** (1966) 104.

[14] M. Cvetic and P. Langacker, *Phys. Rev.* **D46** (1992) 4943; E: ibid. **D48** (1993) 4484.